Introduction

Schoenberg (1980) proposed the linear slip boundary condition to model a non-welded interface. In this model it is assumed that the discontinuity of particle velocity $[\vec{v}]$ can be related to the interface traction $\vec{\tau}_3$ as:

$$[\vec{v}] = i\omega \, \mathbf{Z} \, \vec{\tau}_3; \tag{1}$$

i denoting the imaginary unit and ω the angular frequency. In a 2-D configuration, interface compliance matrix $\mathbf{Z}$ can be written as:

$$\mathbf{Z} = \begin{pmatrix} Z_T & Z_C \\ Z_C & Z_N \end{pmatrix}; \tag{2}$$

Z_N being the normal compliance and Z_T the tangential compliance; cross-coupled compliance Z_C was supplemented by Nakagawa *et al.* (2000). Hudson and Liu (1999) interpreted a fault as a planar distribution of cracks; thus relating the slip to physical properties. Alternatively we can represent a fault zone as a thin layer of cracked material. We show how fault properties such as crack density, crack infill, fault thickness and fault roughness are related to the complex-valued seismic reflection coefficients at the fault surface and how some of these properties can be estimated from these reflection coefficients.

Fault model

We model a fault as a thin layer of cracked material with crack density e , crack radius a and fault thickness h, being small compared to the seismic wavelength. We define crack intensity ζ as:

$$\zeta = e \, h \left(1 + \frac{4\pi}{3} \left(\frac{h}{a} \, e \right)^{\frac{3}{2}} \right). \tag{3}$$

Note that $\zeta \approx e \, h$, corrected by a term that accounts for crack interactions. We follow Hudson and Liu (1999) to relate the tangential compliance to the crack intensity:

$$Z_T = \frac{16\bar{\alpha}^2}{3\bar{\rho} \, \bar{\beta}^2 \, \left(3\bar{\alpha}^2 - 2\bar{\beta}^2\right)} \, \zeta; \tag{4}$$

$\bar{\alpha}$, $\bar{\beta}$ and $\bar{\rho}$ being the P-wave velocity, S-wave velocity and density, respectively, of upper and lower media averaged. It is assumed that the normal compliance relates to the infill of the cracks and the cross-coupled compliance to the presence of micro-corrugations at the fault plane. We define fluid indicator κ as the ratio $\kappa = Z_N/Z_T$, relating to the fluid saturation: $\kappa = 0$ for 100% fluid saturated cracks, whereas $\kappa = 1 - \nu/2$ (ν being the Poisson's ratio) for 100% gas saturated cracks (Shaw and Sen, 2006). Similarly, we define roughness indicator ς as the ratio $\varsigma = Z_C/Z_T$. The compliance matrix can thus be formulated for a 2-D configuration as:

$$\begin{pmatrix} Z_T & Z_C \\ Z_C & Z_N \end{pmatrix} = \frac{16\bar{\alpha}^2}{3\bar{\rho} \, \bar{\beta}^2 \, \left(3\bar{\alpha}^2 - 2\bar{\beta}^2\right)} \begin{pmatrix} \zeta & \varsigma \, \zeta \\ \varsigma \, \zeta & \kappa \, \zeta \end{pmatrix}. \tag{5}$$

Reflection model

We perform Fourier transformation of time and the lateral coordinates and formulate an ordinary differential equation for general anisotropic media (Woodhouse, 1974):

$$\partial_3 \begin{pmatrix} \vec{v} \\ \vec{\tau}_3 \end{pmatrix} = \mathbf{A} \begin{pmatrix} \vec{v} \\ \vec{\tau}_3 \end{pmatrix}. \tag{6}$$

An eigenvalue decomposition is applied:

$$\mathbf{A} = \mathbf{L} \, \mathbf{\Lambda} \, \mathbf{L}^{-1}. \tag{7}$$

$\mathbf{\Lambda}$ holds the eigenvalues that can be related to the vertical wavenumbers of the individual wave modes; composition matrix $\mathbf{L}$ consists of the eigenvectors, relating to the polarizations. Because of this procedure, $\vec{v}$ and $\vec{\tau}_3$ decompose into the down- (indicated with plus sign superscripts) and upgoing (indicated with minus sign superscrips) wave vectors $\vec{w}^{\pm}$:

$$\begin{pmatrix} \vec{v} \\ \vec{\tau}_3 \end{pmatrix} = \mathbf{L} \begin{pmatrix} \vec{w}^{+} \\ \vec{w}^{-} \end{pmatrix}. \tag{8}$$

We scale the system such that the components of $\vec{w}^{\pm}$ represent the particle velocities of the individual wave modes. Consider a downgoing wavefield reflecting at the interface between upper medium I and lower medium II. We distinguish an incident wave field $\vec{w}_I^{+}$, a transmitted wavefield $\vec{w}_{II}^{+}$ and a reflected wave field $\vec{w}_I^{-}$. We define a reflection matrix $\mathbf{R}$ as $\vec{w}_I^{-} = \mathbf{R}\,\vec{w}_I^{+}$ and a transmission matrix $\mathbf{T}$ as $\vec{w}_{II}^{+} = \mathbf{T}\,\vec{w}_I^{+}$. As the components of the wave vectors correspond to the individual wave modes, $\mathbf{R}$ and $\mathbf{T}$ host the reflections and transmissions of the different modes at their diagonals and the converted modes off-diagonal. The non-welded boundary condition can now be formulated as:

$$\mathbf{L}_{II} \begin{pmatrix} \mathbf{T} \\ \mathbf{O} \end{pmatrix} = \begin{pmatrix} \mathbf{I} & i\omega\,\mathbf{Z} \\ \mathbf{O} & \mathbf{I} \end{pmatrix} \mathbf{L}_I \begin{pmatrix} \mathbf{I} \\ \mathbf{R} \end{pmatrix}; \tag{9}$$

$\mathbf{L}_I$ and $\mathbf{L}_{II}$ being the composition matrices of media I and II, respectively. The reflection coefficients of all modes and their conversions can be found by solving this equation for $\mathbf{R}$. Assuming that the interface compliances are small with respect to the medium's background compliance, the reflection coefficient can be approximated as:

$$\mathbf{R} \approx \mathbf{R}_W + i\mathbf{R}_\Psi; \tag{10}$$

$\mathbf{R}_W$ being the reflection coefficient at the welded equivalent of the interface and $\mathbf{R}_\Psi$ being induced by the imperfect interface coupling. Note that both amplitude and phase of a reflecting wavelet are modified. The phase shift of the PP reflection coefficient ϕ^{PP} can be computed through: $\sin\phi^{PP} = R_\Psi^{PP}/|R^{PP}|$. If $R_\Psi^{PP} << |R^{PP}|$, this can be approximated as: $\phi^{PP} \approx R_\Psi^{PP}/|R^{PP}|$. Similar expressions hold for the other wave modes and their conversions.

Inversion at normal incidence

At normal incidence the reflection coefficient matrix $\mathbf{R}$ is defined as the reflection intercept matrix $\mathbf{A}$, with $\mathbf{A} \approx \mathbf{A}_W + i\mathbf{A}_\Psi$ (as in equation 10). The components of $\mathbf{A}_\Psi$ can be related directly to the interface compliances. For P-waves in a 2-D configuration we find:

$$A_\Psi^{PP} = -\left(\frac{1}{\rho_I\,\alpha_I} + \frac{1}{\rho_{II}\,\alpha_{II}}\right)^{-1} (1 - A_W^{PP})\,\omega Z_N. \tag{11}$$

Similarly for S-waves:

$$A_\Psi^{SS} = -\left(\frac{1}{\rho_I\,\beta_I} + \frac{1}{\rho_{II}\,\beta_{II}}\right)^{-1} (1 - A_W^{SS})\,\omega Z_T; \tag{12}$$

and for P-to-S converted waves:

$$A_\Psi^{SP} = -\left(\frac{1}{\rho_I\,\beta_I} + \frac{1}{\rho_{II}\,\beta_{II}}\right)^{-1} (1 - A_W^{PP})\,\omega Z_C. \tag{13}$$

These equations can also be interpreted as approximations of the reflection coefficients of Chaisri and Krebes (2000), evaluated at normal incidence. The compliances can thus be obtained from complex-valued reflection coefficients, that can be retrieved from magnitude and phase of a reflecting wavelet. The compliances can then be related to fault properties through equation 5.

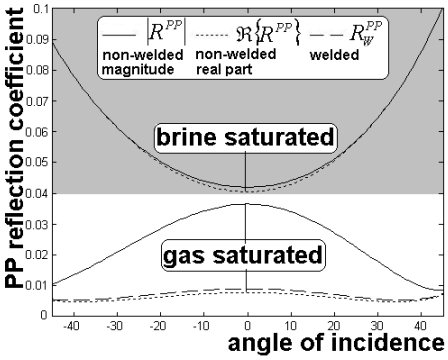

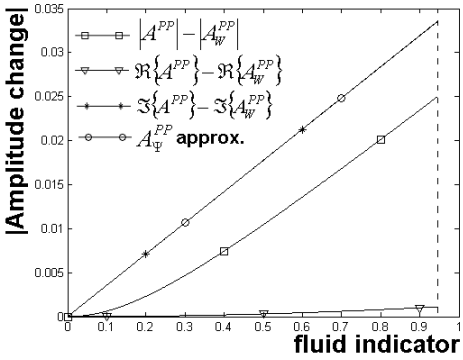

Figure 1: (left panel) Amplitude Variations with Angle (AVA) for brine and gas saturated models, evaluated with either a welded or a non-welded interface at 30 Hz frequency.

Figure 2: (right panel) Change of magnitude, real part and imaginary part of the PP reflection intercept with respect to the PP reflection intercept at the welded equivalent of the interface and the linear relation 11 that we derived for the imaginary part; evaluated with varying fluid indicator κ for $\zeta = 0.3$ without micro-corrugations at 30 Hz frequency; the dotted line represents the gas saturated state, where we neglected crack interaction effects.

The complex-valued PP reflection coefficient can be related to the normal compliance, being an indicator for the fluid saturation. The complex-valued SS reflection coefficient can be related to the tangential compliance, being an indicator for the crack intensity. P-to-S conversion can be used as an indicator for micro-corrugations at the fault plane. As $\mathbf{A}_W^{SP} = 0$, the cross coupled compliance can be retrieved directly from the magnitude of any P-to-S converted wave at normal incidence.

Example

We compute seismic reflection coefficients at a fault that cuts through tight sands with a 30 degrees dip. Both upper and lower media are transverse isotropic with a vertical axis of symmetry (VTI); the contrast being small (samples G13 and G14 of Wang (2002)). We rotate the coordinate system over 30 degrees, such that the fault is placed horizontally in a TTI (transverse isotropic with a tilted axis of symmetry) background. The crack intensity is taken as $\zeta = 0.3$ and the fluid indicator is computed through a formulation of Shaw and Sen (2006), where the average crack aspect ratio is assumed to be $\bar{f} = 0.05$, yielding $\kappa^{BRINE} \approx 0.32$ and $\kappa^{GAS} \approx 0.91$. We compute the Amplitude Variations with Angle (AVA) of the PP reflection upon solving boundary condition 9 for both the brine and gas saturated states (Figure 1). We also show the real part and the response of an equivalent welded interface. The effects of imperfect interface coupling are best exposed at normal incidence. As they are mostly related to the normal compliance, the gas saturated state, with Z_N being large, is more sensitive than the brine saturated state, with Z_N being small. We focus on reflections at normal incidence, where we keep the background constant, with elastic coefficients as in the gas saturated state. In Figure 2 we show the changes in magnitude, real part and imaginary part of the PP reflection intercept with respect to the reflection intercept of an equivalent welded interface, for varying fluid indicators. We also show the result of equation 11, matching perfectly with the imaginary part of the PP reflection intercept. In Figure 3 we show the changes of the SS reflection intercept with varying crack intensity; the results of equation 12 matching perfect with the imaginary part. Figure 4 shows the changes of the P-to-S reflection intercept with varying roughness indicator. As its real part is hardly significant, both imaginary part and magnitude are similar and well described by equation 13.

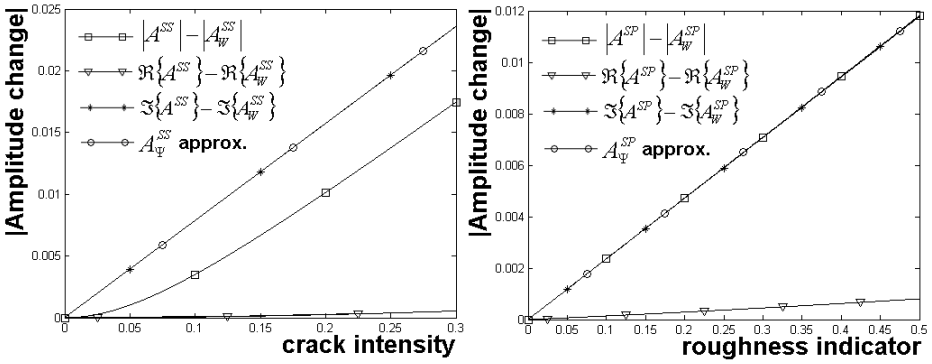

Figure 3: (left panel) Change of magnitude, real part and imaginary part of the SS reflection intercept with respect to the SS reflection intercept at the welded equivalent of the interface and the linear relation 12 that we derived for the imaginary part; evaluated for gas saturated cracks with varying crack intensity ζ without micro-corrugations at 30 Hz frequency.

Figure 4: (right panel) Change of magnitude, real part and imaginary part of the P-to-S reflection intercept with respect to the P-to-S reflection intercept at the welded equivalent of the interface and the linear relation 13 that we derived for the imaginary part; evaluated for gas saturated cracks and $\zeta = 0.3$ with varying roughness indicator ς at 30 Hz frequency.

Conclusion

Both magnitude and phase of seismic reflection coefficients at a fault can reveal important information on the fault properties. The complex-valued reflection coefficients can be retrieved by extracting the phase from the shape of a reflecting wavelet. PP reflection coefficients can be used for gas / fluid identification, whereas SS reflection coefficients characterize the crack intensity - a product of crack density and fault thickness, with a correction term for crack interactions. Finally, PS conversion at normal incidence can reveal the presence of micro-corrugations at the fault plane.

References

Chaisri, S., and Krebes, E. S.[2000] Exact and approximate formulas for p-sv reflection and transmission coefficients for a nonwelded contact interface. *Journal of Geophysical research* 105, 28.045–28.054.

Hudson, J. A., and Liu, E.[1999] Effective elastic properties of heavily faulted structures. *Geophysics* 64, 479–485.

Nakagawa, S., Nihei, K. T. and Myer, L. R.[2000] Shear-induced conversion of seismic waves across single fractures. *International Journal of Rock Mechanics and Mining Sciences* 37, 203–218.

Schoenberg, M. [1980] Elastic wave behavior across linear slip interfaces. *Journal of the Acoustical Society of America* 68, 1516–1521.

Shaw, R. K., and Sen, M. K.[2006] Use of avoa data to estimate fluid indicator in a vertically fractured medium. *Geophysics* 71, C15–C24.

Wang, Z. [2002] Seismic anisotropy in sedimentary rocks, part 2: Laboratory data. *Geophysics* 67, 1423–1440.

Woodhouse, J. H. [1974] Surface waves in a laterally varying layered structure. *Geophysical Journal of the Royal Astronomical Society* 37, 461–490.